České vysoké učení technické v Praze, Fakulta elektrotechnická
Czech Technical University in Prague, Faculty of Electrical Engineering

doc. Ing. Jan Sýkora, CSc.

Modulace, kódování a zpracování signálu v MIMO rádiových komunikačních systémech

Modulation, Coding and Signal Processing in MIMO Radio Communication Systems

Summary

The text first provides a brief introduction into the theory of the space-time modulation, coding and signal processing for MIMO (Multiple-Input Multiple-Output) channel. Then, we focus in more detail on the nonlinear space-time modulation, coding and nonlinear receiver signal processing in MIMO systems. We show the results for information theoretic limits of the finite alphabet nonlinear space-time modulation in MIMO channel. We develop trellis code design rules for the nonlinear space-time modulation. Finally, we concentrate on the nonlinear processing of the space-time CPM signals in MIMO channel. Particularly we develop Information Waveform Manifold (IWM) based signal preprocessing. We analyze its information efficiency and the multiplexing properties of the IWM based discriminator.

Souhrn

Text nejprve poskytuje stručný úvod do problematiky časo-prostorových modulací, kódování a zpracování signálu pro MIMO (Multiple-Input Multiple-Output) kanál. Následně se podrobně zabýváme problematikou nelineárních časo-prostorových modulací, kódování a nelineárního zpracování signálu pro MIMO systémy. Předkládáme výsledky pro informačně teoretické limity nelineární časo-prostorové modulace s konečnou abecedou v MIMO kanálu. Dále ukazujeme metody návrhu mřížkového kódu pro nelineární časo-prostorové modulace. V závěru se zabýváme nelineárním zpracováním časo-prostorových CPM signálů v MIMO kanálu. Zejména se jedná o zpracování signálu založené na IWM (Information Waveform Manifold) přístupu. Analyzujeme jeho informačně teoretickou účinnost a multiplexní vlastnosti IWM diskriminátoru.

Keywords

MIMO communication systems, nonlinear space-time modulation, coding, nonlinear signal processing

Klíčová slova

MIMO komunikační systémy, nelineární časo-prostorové modulace, kódování, nelineární zpracování signálu

©Jan Sykora
R1.0.0 (16.9.2006)
ISBN

Contents

1 Introduction and Motivation

1.1 Motivation

Physical layer processing algorithms (modulation, coding, signal processing, synchronization, equalization) are the most critical part of the radio communication system. They directly influence the effectiveness and performance of the utilization of very sparse natural resource — the radio spectrum. Any fault or deficiency on the physical layer processing design is highly paid by decreased performance and low utilization of the propagation medium.

Decades of effort were devoted to the search of better modulation, coding, more effective receiver signal processing. But only at the end of the last decade, there appeared a new breakthrough. It was the appearance of the idea of having multiple antennas both on transmitter and receiver part together with dedicated multichannel Space-Time (ST) modulation, coding and signal processing. It was shown that such Multiple-Input Multiple-Output (MIMO) system has much higher information capacity and reliability comparing to the traditional scalar system. This was a start of enormous research activity taking a new fresh wind into the radio mobile communications.

1.2 Current state of art

The research activity in the area of Space-Time Coded (STC) modulations for MIMO communication systems attracted a lot of attention in recent years. A huge number of results is already available (see e.g. [1] and the references therein). The topic is investigated from number of viewpoints starting with the channel capacity evaluation (see e.g. [2], [3]) and going into the synthesis of the space-time modulation (e.g. [4]) and demodulation, detection and synchronization signal processing algorithms [1], [5].

1.3 Nonlinear ST modulation, coding and signal processing

A vast majority of the research results in MIMO communications however focused so far on the *linear* modulations, coding and signal processing methods. The reasons for that are various, but one of the most important is their relatively easy mathematical tractability. On the other side, *nonlinear* modulations, coding and signal processing provide some very attractive benefits (see e.g. [6], [7], [8], [9]).

One of the most attractive features is the ability of nonlinear modulation to better respect technology constraints of the practical communication system. Particularly, it is the technology constraint on the transmitter side (e.g. the nonlinear C-class amplifier). The nonlinear modulation is better suited to this situation due to its ability to put additional waveform constraints on the signal. The most important property is the resistance to nonlinear distortion for *constant envelope* class of modulations Space-Time CPM. We also have more degrees of freedom and ability to decouple the constellation 2-nd order properties (distances) and actual waveform shape reflecting the transmitter technology constraints. This opens wide possibilities for the space-time code design.

On the receiver side, the most problematic technology constraint is the limited computational power available for the signal processing. The price paid for having more degrees of freedom on transmitter side is in the higher waveform dimensionality of the nonlinearly modulated signal which increases the complexity of the receiver processing. On the receiver side, there is also a number of processing and technology constraint areas that can effectively benefit from the nonlinear modulation, e.g. the limiter receiver type and simplification of the receiver

gain control. A *nonlinear* receiver preprocessing for ST-CPM is a very effective way to reduce the complexity of the receiver signal processing by reducing the dimensionality of the problem and it can also directly address the constraints of the receiver processing path.

IWM based nonlinear preprocessing for CPM class NSTM is, apart of reducing the dimensionality of the problem, providing one very special feature — capability of *separating* the signals from individual transmitters *without the necessity of any time-domain processing*. Everything is achieved only in value-domain. This is a very specific feature particular only to nonlinear modulations with IWM processing *not possible* with traditional linear signal space processing approach. We analyze multiplexing properties of the IWM phase discriminator based on information-theoretic capacity region approach (see Sec. 6.8).

1.4 Outline of the text

Chapter 2 serves as a gentle introduction into the field of MIMO systems, modulation and coding. We provide simplified view of a quite diverse and complicated area in a form suitable for the reader not particularly being expert in the field.

Chapter 3 defines Nonlinear Space-Time Modulation (NSTM) and develops a suitable channel model and multidimensional waveform space description. Chapter 4 analyzes the fundamental information theoretic limits of the finite alphabet NSTM in MIMO system. Chapter 5 synthesizes a method of ST trellis coding for NSTM in Rayleigh MIMO channel. Chapter 6 develops nonlinear Information Waveform Manifold (IWM) based receiver signal processing for NSTM of the CPM type. Besides an explanation of the novel IWM approach, the essential IWM processing properties are analyzed — the information transfer efficiency and the multiplexing capabilities of the IWM discriminator.

Chapters 3, 4, 5, 6 form the *core of the text* and present *author's particular field of the research expertise*. Most of the results, particularly in Chapters 4, 5, 6 present a cutting-edge research results. Especially the *nonlinear processing* in Chapter 6 is author's unique contribution not being developed by any other author so far.

2 MIMO Radio Communication System

2.1 System model

Spatial diversity MIMO (Multiple-Input Multiple-Output) communication system is generally a communication system using a multidimensional channel where the channel dimensionality is physically resolved in spatial dimensions. This is usually achieved by a multi-element antenna arrays having a capability of distinguishing signals to/from various spatial angles by proper space-time signal processing.

Each pair of transmit and receive antenna forms one component communication channel. Depending on the particular properties of communication propagation media, it can be modeled as time-variant or time-invariant, frequency selective or non-selective, stochastic or deterministic, etc., see [10], [11]. For the purpose of this introductory chapter, we constrain ourselves to the most common channel type — randomly block-fading frequency non-selective Rayleigh channel. In this type of channel the input-output equation is

$$\begin{bmatrix} x_1(t) \\ \vdots \\ x_{N_R}(t) \end{bmatrix} = \begin{bmatrix} h_{11} & \dots & h_{1N_T} \\ \vdots & & \vdots \\ h_{N_R} & \dots & h_{N_R N_T} \end{bmatrix} \begin{bmatrix} s_1(t) \\ \vdots \\ s_{N_T}(t) \end{bmatrix} + \begin{bmatrix} w_1(t) \\ \vdots \\ w_{N_R}(t) \end{bmatrix} \tag{1}$$

where N_T, N_R is the number of transmit and receive antennas respectively, $s_i(t)$ is the transmitted signal in ith antenna, $x_k(t)$ is the received signal in kth antenna and $w_k(t)$ is the additive Gaussian noise (AWGN). The channel coefficients are constant for the block length $t \in [0, T]$ and forms the channel matrix $\mathbf{H}$.

Time domain system description is fundamental, however the design of the Space-Time Coding (STC) and investigation of the fundamental system limits requires easier to handle description. This is the waveform space model (see [12], [10]). Its inputs are directly the constellation points of the codeword symbols $\mathbf{s}_n$ and the receive signal is the matched filter projection of the signal in time domain. In this chapter, we assume a *linear* modulation where the (complex) dimension of the constellation point per one spatial dimension is equal to 1. The case of *nonlinear* modulation will be treated in subsequent chapters in more detail. The waveform space signal input-output model is

$$\mathbf{x}_n = \mathbf{H}\mathbf{s}_n + \mathbf{w}_n, \quad n \in \{1, 2, \dots, N\} \tag{2}$$

where $\mathbf{s}_n$ is N_T dimensional spatial constellation point for nth symbol in the sequence, $\mathbf{x}_n, \mathbf{w}_n$ are N_R dimensional projections of the received signal and AWGN into waveform constellation space. The basis used for the projection of the signal into the waveform constellation space is assumed to be Nyquist and orhonormal.

2.2 Fundamental limits

2.2.1 Channel capacity

One of the major attractions of the MIMO system is the increase of the information capacity of the system. The underlying principle, shared in all flavors of the MIMO channels, is based on our capability of transforming the channel into *parallel orthogonal* information streams. This is mathematically done by Singular Value Decomposition (SVD) of the channel matrix

$$\mathbf{H} = \mathbf{U}\mathbf{D}\mathbf{V}^H. \tag{3}$$

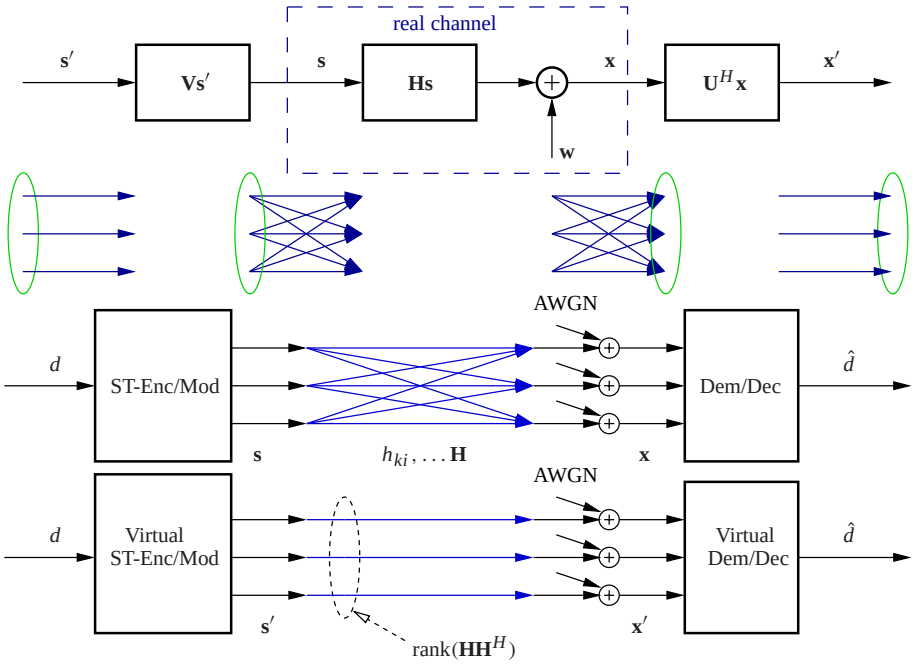

Figure 1: Channel eigenmodes.

$\mathbf{U}$, $\mathbf{V}$ are unitary matrices ($\mathbf{U}^H\mathbf{U} = \mathbf{I}$). Subsequently, we can formulate a new equivalent input-output relationship of the channel

$$\underbrace{\mathbf{U}^H\mathbf{x}}_{\mathbf{x}'} = \mathbf{D}\underbrace{\mathbf{V}^H\mathbf{s}}_{\mathbf{s}'} + \underbrace{\mathbf{U}^H\mathbf{w}}_{\mathbf{w}'}, \tag{4}$$

$$\mathbf{x}' = \mathbf{D}\mathbf{s}' + \mathbf{w}'. \tag{5}$$

This form of the model model is called channel eigenmodes since the matrix of the eigenvalue square roots is diagonal $\mathbf{D} = \mathrm{diag}(\ldots, \sqrt{\mathrm{eig}_i(\mathbf{H}\mathbf{H}^H)}, \ldots)$ and it effectively transforms the channel into parallel sub-channels. The number of parallel paths is given by the channel matrix rank. See Fig. 1.

The MIMO channel capacity can be shown to be a sum of capacities of sub-channels

$$C = \sum_{i=1}^{N_H} \log_2\left(1 + \frac{\lambda_i}{N_T}\gamma\right) \quad \text{[bit/s/Hz]} \tag{6}$$

under slightly simplifying assumptions of deterministic channel with $N_H = \mathrm{rank}(\mathbf{H}\mathbf{H}^H)$, $\lambda_i = \mathrm{eig}(\mathbf{H}\mathbf{H}^H)_i$. The $\gamma = \bar{\mathcal{E}}_S/\sigma_w^2$ is the signal to noise ratio (SNR) where $\bar{\mathcal{E}}_S$ is mean total symbol energy, σ_w^2 is the AWGN variance per receiver. Compare this capacity with the capacity of traditional scalar channel

$$C = \log_2(1+\gamma) \quad \text{[bit/s/Hz]}. \tag{7}$$

We observe that the MIMO capacity scales logarithmically with the SNR the same way as for the scalar channel. There is additional Rx antenna array gain represented through λ_i values. However, the most important is the fact, that it also scales *linearly* with the channel rank which is in turn given by the number of antennas and particular propagation environment. The linear scaling with number of antennas holds (under some assumptions) also for random channel (see the next chapters). It is very important to stress that this capacity increase is *under the same spectral and power limitations*, i.e. the total transmitted power and spectrum occupied are the same. The increase is purely due to increased number of antennas.

2.2.2 Diversity

The diversity of the system is a measure of its capability do deliver the information over the independent paths. Those paths must be resolvable, i.e. the system capabilities must be such that the individual path can be separated by suitable signal processing. The diversity can be achieved in (absolute) time, relative (delay) time domain (frequency diversity), and spatial domain (multiple antennas). The MIMO (N_T, N_R) system achieves at maximum the spatial diversity of the order $L = N_T N_R$. This situation is referred to as *full spatial diversity* system. The particular code that allows to achieve that is called the full spatial diversity code. Diversity properties of the code are given by the minimum rank of the codeword difference Gram matrix over all data message pairs

$$[\mathbf{R}_c^{(a,b)}]_{ij} = \int_{-\infty}^{\infty} (s_i(t, \mathbf{d}^{(a)}) - s_i(t, \mathbf{d}^{(b)}))^* (s_j(t, \mathbf{d}^{(a)}) - s_j(t, \mathbf{d}^{(b)}))\, dt, \quad i, j \in \{1, \ldots, N_T\}. \tag{8}$$

The diversity order of the code is $L = N_R \min_{a,b} \operatorname{rank} \mathbf{R}^{(a,b)}$.

2.3 Space-Time Modulation and Coding

A Space-Time Coder performs coding in N_T parallel streams that subsequently feed the N_T modulators. Typically those modulators are of the same type, e.g. all using linear modulation with the same constellation alphabet. In the special case of linear modulation (the advanced case of nonlinear modulation is treated later) we have

$$\mathbf{s}(t) = \begin{bmatrix} s_1(t) \\ \vdots \\ s_{N_T}(t) \end{bmatrix} = \sum_n \begin{bmatrix} q_{1,n} \\ \vdots \\ q_{N_T,n} \end{bmatrix} g(t - nT_S) \tag{9}$$

where $\vec{\mathbf{q}}(\mathbf{d}) = [\ldots, \mathbf{q}_n, \ldots]$ the multidimensional space-time codeword, $\mathbf{d}$ is the vector of data, and $g(.)$ is the modulation impulse. The actual space-time code is the mapping $\mathbf{d} \mapsto \vec{\mathbf{q}}$.

Depending on the particular form of the mapping $\mathbf{d} \mapsto \vec{\mathbf{q}}$ we classify the codes into the following classes STTC (Space-Time Trellis-Code), STBC (Space-Time Block-Code), LSTC (Layered Space-Time Code).

2.3.1 Diversity and coding gain

A performance of the STC is assessed through two basic criteria — diversity and coding gain. Under some simplifying condition, we can show that the probability of detection error is generally following the rule

$$P_e(\lambda) \approx P_{e0} e^{-\lambda \gamma \Gamma_c / 2} \tag{10}$$

where P_{e0} is the linear scaling factor, Γ_c is the coding gain, λ is the composite power transfer of the propagation path and γ is the mean SNR.

Average error probability in random Rayleigh channel is averaged over the PDF of the channel transfer

$$\bar{P}_e = \int_0^{\infty} P_e(\lambda)\, p(\lambda)\, d\lambda. \tag{11}$$

The particular form of the $p(\lambda)$ depends on particular code and signal processing used. Value λ represents combined transfer of all L existing paths of the Lth order diversity system. The combination can be either explicit (e.g. Maximum Ratio Combining) or implicit through proper

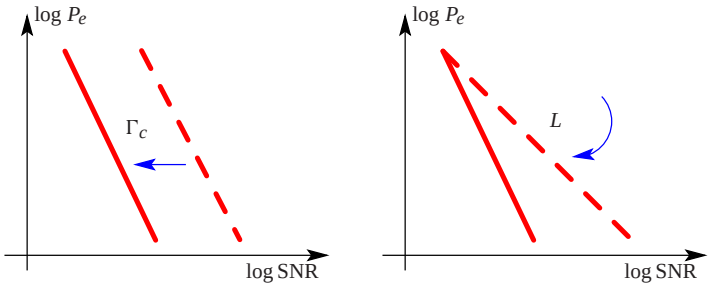

Figure 2: Diversity and coding gain.

processing of the STC. The composite path has χ^2 distribution with $2L$ degrees of freedom. The mean error probability is then

$$\bar{P}_e = P_{eo}(1+\gamma\Gamma_c)^{-L}. \tag{12}$$

We see that the diversity order increases the slope of the error curve while coding gain shifts the curve in horizontal direction (Fig. 2).

For a slowly fading Rayleigh channel, the coding gain can be shown, under some simplifying conditions, to be proportional to the product of nonzero eigenvalues $\Pi_i \lambda_i$. The code design rule based on maximizing this is called determinant criterion [4].

2.3.2 Block space-time codes

Here, we present only a very basic STBC — the Alamouti code, the keystone of all codes based on Orthogonal Design (OD). It will serve well for clarifying the idea behind.

The code uses $N_T = 2$ Tx antennas and the block lengths is $N = 2$. It creates an orthogonal codeword matrix

$$\mathbf{Q} = \begin{bmatrix} d_1 & -d_2^* \\ d_2 & d_1^* \end{bmatrix} \begin{matrix} \downarrow \text{space} \\ \rightarrow \text{time} \end{matrix}, \qquad \mathbf{Q}^H\mathbf{Q} = \begin{bmatrix} |d_1|^2+|d_2|^2 & 0 \\ 0 & |d_1|^2+|d_2|^2 \end{bmatrix}. \tag{13}$$

The decision metric of the decoder in the MIMO $(2,2)$ case is obtained with the help of properly stacked receive symbols

$$\underbrace{\begin{bmatrix} x_{0,1} \\ x_{1,1}^* \\ x_{0,2} \\ x_{1,2}^* \end{bmatrix}}_{\tilde{\mathbf{x}}} = \underbrace{\begin{bmatrix} h_{11} & h_{12} \\ h_{12}^* & -h_{11}^* \\ h_{21} & h_{22} \\ h_{22}^* & -h_{21}^* \end{bmatrix}}_{\tilde{\mathbf{H}}} \underbrace{\begin{bmatrix} d_0 \\ d_1 \end{bmatrix}}_{\mathbf{d}} + \underbrace{\begin{bmatrix} w_{0,1} \\ w_{0,2}^* \\ w_{1,1} \\ w_{1,2}^* \end{bmatrix}}_{\tilde{\mathbf{w}}}. \tag{14}$$

Equivalent channel matrix $\tilde{\mathbf{H}}$ shares the same structure as original Alamouti codeword and it is orthogonal

$$\tilde{\mathbf{H}}^H\tilde{\mathbf{H}} = \begin{bmatrix} \sum_{ik}|h_{ki}|^2 & 0 \\ 0 & \sum_{ik}|h_{ki}|^2 \end{bmatrix} = \sum_{ik}|h_{ki}|^2\mathbf{I}_2. \tag{15}$$

The decoding metric is obtained by

$$\mathbf{z} = \tilde{\mathbf{H}}^H\tilde{\mathbf{x}} = \sum_{ik}|h_{ki}|^2\mathbf{d}^\ell + \mathbf{w}^\ell \tag{16}$$

This output is equivalent to the *virtual scalar channel* with AWGN and with *equivalent gain* $\sum_{ik}|h_{ki}|^2$. We clearly see that the system has *full diversity order* 4.

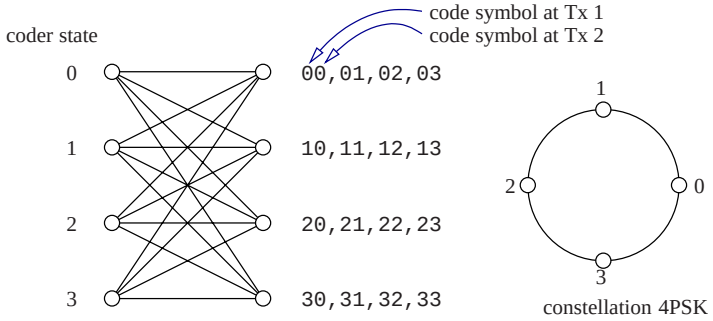

Figure 3: 2-space, 4-state, 4PSK Tarokh's ST-TC.

2.3.3 Trellis space-time codes

The Space-Time Trellis Coded (ST-TC) modulation uses a trellis based description of the coding algorithm. The code produced is characterized by having unity rate. This guarantees no bandwidth expansion over the uncoded system — there is one channel symbol per one incoming data symbol. The *redundancy* of the channel symbol set is purely achieved by the *expansion* of the *alphabet* used and not by the waveform dimension increase of the channel symbols.

The simplest possible example of such a code is original Tarokh's 2-space, 4-state, 4PSK code [4]. The code in fact artificially creates diversity in delay. The ST-TC can be optimized for various channel types. ST trellis codes can have full diversity order and quite large coding gains, that increase with number of the coder states. A large number of the codes can be found in [1]. The decoding of the ST-TC must be (due to a presence of the memory) done through trellis path search algorithms. The most typical is the Viterbi Algorithm.

3 Nonlinear Space-Time Modulation and Coding

3.1 Nonlinear space-time modulator

The Nonlinear Space-Time Modulation (NSTM) generates *nonlinearly* modulated signal at each transmitter antenna. The complex envelope signal on i-th transmit antenna is

$$s_i(t) = \sum_n g(q_{n,i}, t - nT_S) \tag{17}$$

where T_S is the symbol period, $g(q_{n,i}, t)$ is generally *nonlinear* modulation waveform, $q_{n,i} \in \{q^{(m)}\}_{m=1}^{M_q}$ is a channel symbol and n is its sequence number. The channel symbol depends on the modulator input data $c_{n,i} \in \{c^{(m)}\}_{m=1}^{M_c}$ and modulator state $\sigma_{n,i} \in \{\sigma^{(m)}\}_{m=1}^{M_\sigma}$ through time-invariant generally *nonlinear* function $q_{n,i} = q_i(c_{n,i}, \sigma_{n,i})$. M_q, M_c, M_σ are alphabet (per-transmitter) sizes for channel symbol, input codeword, and modulator state respectively.

The function $q_i(c_{n,i}, \sigma_{n,i})$ forms a discrete part of the modulator. It can be fully described by the Finite State Machine (FSM) model. The function $g(q, t)$ forms an expansion part (discrete input, continuous waveform output) of the modulator. The set of all possible modulator expansion part output waveforms is $g(\cdot, t) \in \{g^{(m)}(t)\}_{m=1}^{M_q}$. The modulation functions are assumed to be Nyquist ones. This guarantees that the expansion part is memoryless. Modulators (discrete and expansion parts) in individual transmitter branches are independent and identical.

3.2 Waveform and memory constraint

A proper choice of the discrete and expansion part of the modulator can be used to constrain waveform and memory behavior of the signal. The most typical waveform constraint is the constant envelope one. As an additional tool, the memory constraint can be imposed (affecting mainly spectral properties). The most typical one is the continuous signal constraint. As an practically important example, the *CPM class of constant envelope modulation* uses both of the above mentioned.

A capability of having more degrees of freedom for imposing additional waveform and memory constraints is *particular* to nonlinear modulations only. It allows to decouple waveform and memory properties from the second order distance properties (affecting BER properties). Linear modulations are severely limited in this aspect.

Modulator constraint—waveform only, IID channel symbols The constraint on the set of waveforms $g(\mathbf{.}, t) \in \{g^{(m)}(t)\}_{m=1}^{M_q}$ available through the set of channel symbols $q_{n,i} \in \{q^{(m)}\}_{m=1}^{M_q}$ is the *fundamental* one that controls the *class* of used *channel waveforms* (e.g. the *constant envelope* ones).

Modulator constraint—waveform and memory The mapping $c_{n,i} \mapsto q_{n,i}$ puts an additional *optional* constraint related to the *memory* of modulation. It is useful to impose e.g. the *continuity of the phase* which could not be modeled otherwise. Assuming $(c_{n,i}, \sigma_{n,i}) \mapsto q_{n,i}$ being a *one-to-one* mapping, the sequence $\{q_{n,i}\}_n$ forms a *stationary* Markov chain.

3.3 Channel

The channel is considered to be frequency flat block-constant fading (N_T, N_R) MIMO channel with AWGN (Additive White Gaussian Noise). A received signal at k-th receive antenna is

$$x_k(t) = \sum_{i=1}^{N_T} h_{ki} s_i(t) + w_k(t) \tag{18}$$

where h_{ki} are channel coefficients and $\{w_k(t)\}_{k=1}^{N_R}$ are IID zero mean rotationally invariant complex white Gaussian noise processes with power spectrum density $S_w(f) = 2N_0$. Channel coefficients are zero mean IID complex Gaussian random variables with unity variance $\mathrm{E}[|h_{ki}|^2] = 1$. We also form a $(N_R \times N_T)$ channel matrix $[\mathbf{H}]_{ki} = h_{ki}$.

3.4 Multidimensional constellation waveform space model

Arbitrary nonlinear modulation can be equivalently expressed using multidimensional waveform Euclidean signal space representation of the waveform corresponding to the n-th symbol at one antenna

$$g(q_{n,i}, t) = \mathbf{s}_{n,i}^T \mathbf{g}(t). \tag{19}$$

The vector $\mathbf{s}_{n,i} = [s_{n,i,1}, \ldots, s_{n,i,N_s}]^T$ is the N_s dimensional signal space representation of the waveform (constellation point) and $\mathbf{g}(t) = [g_1(t), \ldots, g_{N_s}(t)]^T$ is vector of *orthonormal* and *Nyquist* basis functions. The space spanned by $\mathbf{g}(t)$ is called *constellation (waveform) space*. In a special case of linear modulation, the dimension is $N_s = 1$. For nonlinear modulation, this is however $N_s > 1$. The constellation points can be get e.g. by Gram-Schmidt procedure or

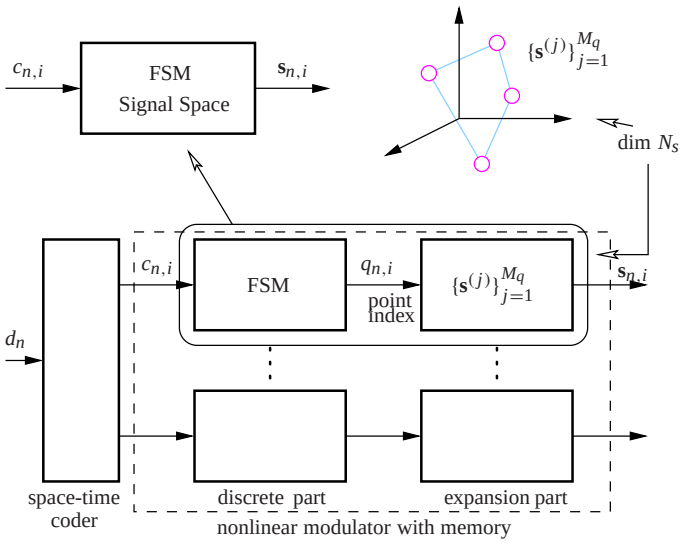

Figure 4: Multidimensional constellation waveform space model of NSTM.

by informationally equivalent decomposition [9]. The constellation points are selected by the output of the FSM $q_{n,i} = q_i(c_{n,i}, \sigma_{n,i})$ (Fig. 4).

An alternative to the orthonormal and Nyquist waveform space basis is the Laurent decomposition [13]. It also produces linear expansion of the waveform. However, it possesses one very important deficiency — the Laurent decomposition (including the tilted phase variants) *does not* produce orthonormal nor Nyquist basis. The orthonormality and Nyquist property is a very important feature from the point of view of the code design and also for the receiver signal processing (particularly the receiver metric evaluation).

The fact that the nonlinear modulation has waveform dimensionality $N_s > 1$ has a number of positive consequences. It opens additional dimensions that can be used for the code design increasing both the capacity and the potential diversity gain. See [12] and [9] for details.

3.5 Waveform Space channel model for NSTM

The received signal at k-th receive antenna (dimensionality N_s per antenna) in signal space notation is

$$\mathbf{x}_{n,k} = \sum_{i=1}^{N_T} h_{ki}\mathbf{s}_{n,i} + \mathbf{w}_{n,k}. \tag{20}$$

This can be written in a compact form using space-stacked vectors and matrices

$$\tilde{\mathbf{x}}_n = \tilde{\mathbf{H}}\tilde{\mathbf{s}}_n + \tilde{\mathbf{w}}_n \tag{21}$$

where $\tilde{\mathbf{x}}_n = [\mathbf{x}_{n,1}^T, \ldots, \mathbf{x}_{n,N_R}^T]^T$ and similarly for $\tilde{\mathbf{s}}_n$ and $\tilde{\mathbf{w}}_n$. The stacked channel matrix has a *Kronecker* structure $\tilde{\mathbf{H}} = \mathbf{H} \otimes \mathbf{I}_{N_s}$ ($\otimes$ is a Kronecker product), see Fig. 5.

Channel eigenmodes

$$\tilde{\mathbf{x}}_n = \tilde{\mathbf{V}}_1\tilde{\mathbf{D}}\tilde{\mathbf{V}}_2^H\tilde{\mathbf{s}}_n + \tilde{\mathbf{w}}_n \tag{22}$$

can be also shown to have a Kronecker structure $\tilde{\mathbf{V}}_1 = \mathbf{V}_1 \otimes \mathbf{I}_{N_s}$, $\tilde{\mathbf{V}}_2 = \mathbf{V}_2 \otimes \mathbf{I}_{N_s}$ $\tilde{\mathbf{D}} = \mathbf{D} \otimes \mathbf{I}_{N_s}$ where $\mathbf{H} = \mathbf{V}_1\mathbf{D}\mathbf{V}_2^H$ is SVD decomposition, $\mathbf{D} = \mathrm{diag}(\ldots, \sqrt{\lambda_i}, \ldots)$ is matrix of eigenvalues.

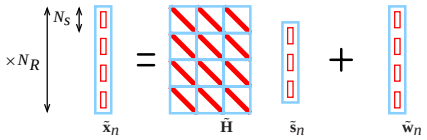

Figure 5: Stacked channel matrix with Kronecker structure.

4 Fundamental limits for NSTM

4.1 Channel capacity of NSTM with multidimensional waveform constellation

The multidimensional waveform constellation increases the channel capacity. Each dimension forms additional orthogonal information channel. This is however paid by increased signal bandwidth. Fortunately, the signal bandwidth grows linearly with the dimension of the signal *only asymptotically*. For signals with moderate dimensionality the grows can be much smaller. Here, we summarize the capacity results for multidimensional waveform constellations (see [12] for details).

4.1.1 Deterministic channel with no TxCSI

We assume that the channel state information is *not available* at the transmitter and only total symbol energy $\bar{\mathcal{E}}_S$ constraint is put in effect. In this case, the symbol energy is split evenly over all spatial branches as well as over dimensions within the waveform constellation

$$\bar{\mathcal{E}}_i = \frac{\bar{\mathcal{E}}_S}{N_T}, \quad \mathrm{E}\left[|s_{i,n}|^2\right] = \frac{\bar{\mathcal{E}}_i}{N_s}. \tag{23}$$

The resulting capacity is

$$C = N_s \sum_{i=1}^{N_H} \log_2\left(1 + \frac{\lambda_i \bar{\mathcal{E}}_S}{N_s N_T \sigma_w^2}\right). \tag{24}$$

Very often, the following formal form of the capacity equation is useful

$$C = N_s \log_2 \det\left(\mathbf{I} + \frac{\bar{\mathcal{E}}_S}{N_s N_T \sigma_w^2}\mathbf{H}\mathbf{H}^H\right). \tag{25}$$

An essential observation that can be drawn from the both cases is that the channel capacity scales *linearly with the rank of the channel* N_H and *dimensionality of symbols*. This means that for a given fixed energy per symbol to noise variance, the MIMO system has great capacity advantage over a scalar system.

4.1.2 Rayleigh IID fading channel

In the previous text, we treated an instantaneous channel capacity for a given channel matrix $\mathbf{H}$. However, for a random fading channel, we are rather interested in the average capacity. Let us assume that the channel is ergodic, i.e. its randomness exhibits itself entirely within the channel observation frame. On this condition, the ergodic average capacity (no CSI at the transmitter) is get by averaging over all channel states

$$\begin{aligned} \bar{C} &= \mathrm{E}_{\mathbf{H}}[C] \\ &= \mathrm{E}_{\mathbf{H}}\left[N_s \log_2 \det\left(\mathbf{I} + \frac{\bar{\mathcal{E}}_S}{N_s N_T \sigma_w^2}\mathbf{H}\mathbf{H}^H\right)\right]. \end{aligned} \tag{26}$$

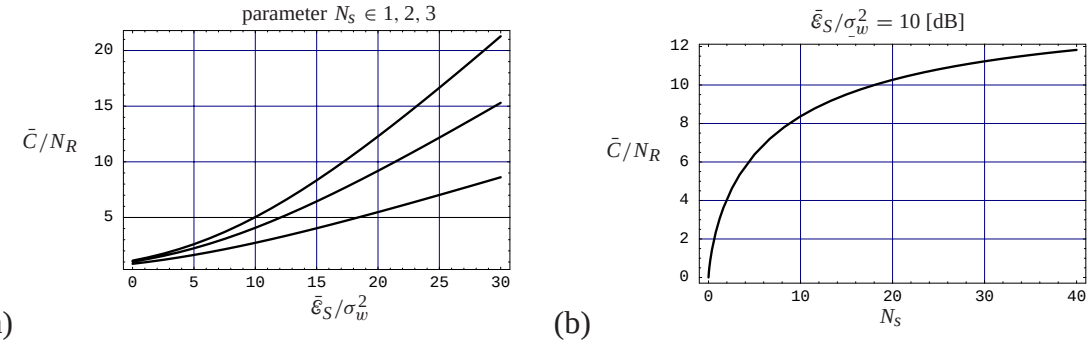

Figure 6: (a) Channel capacity (28) as a function of symbol energy to noise variance ratio. (b) Channel capacity (28) as a function of symbol dimensionality.

In the case of nonergodic channel, we must resort to the outage capacity which is in fact a probability distribution of instantaneous capacity.

The capacity averaging for a general case of arbitrary N_T, N_R is mathematically rather involved task. Details of the derivation can be found in [2]. The resulting expression for IID zero mean complex Gaussian channel transfer coefficients with unity variance is

$$\bar{C} = N_s \int_0^\infty \log_2\left(1 + \frac{\bar{\mathcal{E}}_S \lambda}{N_s N_T \sigma_w^2}\right) \sum_{k=0}^{m-1} \frac{k!}{(k+n-m)!} \left(L_k^{n-m}(\lambda)\right)^2 \lambda^{n-m} e^{-\lambda}\, d\lambda \tag{27}$$

where $m = \min(N_T, N_R)$, $n = \max(N_T, N_R)$ and $L_j^i(\cdot)$ is Laguerre polynomial.

It can be shown [2] that for a special, however significant, case of large $N_T = N_R$ the average capacity per symbol again linearly scales with the dimensionality of the channel

$$\bar{C} = N_s N_R \int_0^4 \log_2\left(1 + \frac{\bar{\mathcal{E}}_S \nu}{N_s \sigma_w^2}\right) \frac{1}{\pi} \sqrt{\frac{1}{\nu} - \frac{1}{4}}\, d\nu. \tag{28}$$

We again see that the capacity grows with waveform space dimension. A graphical representation of this equation is on Fig. 6. It is very important to notice a limiting behavior of its dependence on the symbol dimensionality for a constant mean symbol energy

$$\lim_{N_s \to \infty} \bar{C} = N_R \frac{\bar{\mathcal{E}}_S}{\sigma_w^2 \ln 2}. \tag{29}$$

4.2 Symmetric capacity of finite alphabet NSTM

Fundamental capacity limits of the NSTM, in a *special* but practically important case of *finite symbol alphabet*, can be assessed with the utilization of the informationally equivalent system model (see [9]).

4.2.1 Symmetric capacity

We evaluate the *symmetric capacity* (denoted by C_*). It is defined as the mutual information between channel input and output with the uniform distribution of input symbol probabilities $P_m = P_{m,i} = \Pr\{c_{n,i} = c^{(m)}\} = 1/M_c$ for all i.

The *true* capacity (maximized over all input distributions) is equivalent to the symmetric capacity if the capacity achieving distribution is uniform. It happens in many cases, but unfortunately there is no general way of finding this. We can formulate number of *sufficient* (however

generally not necessary) conditions for this situation. It can be shown [14] (based on a similar arguments as in [11, sec. 7.1.2]) that one of such special situations is the following case of *symmetric* signal set. If the set of all possible signal differences with suitable unitary transformation does not depend on k, i.e.,

$$\forall k \exists \mathbf{U} : \{\mathbf{U}(\mathbf{s}^{(m)} - \mathbf{s}^{(k)})\}_m = \{\mathbf{s}^{(m)} - \mathbf{s}^{(1)}\}_m \tag{30}$$

then the the capacity achieving probability distribution is *uniform* at the level of $\mathbf{s}$ symbols (assuming IID symbols).

In the following, we assume no channel state information at the transmitter and the perfect one at the receiver.

4.2.2 Capacity factorization per one eigenmode

An important *consequence* of our ability (see [9]) to express the finite alphabet channel with equivalent signal space representation of the waveforms directly applied to eigenmodes is the possibility of the capacity factorization per one eigenmode. The total capacity *per one channel symbol* is a sum of capacities per one eigenmode. Assuming identical modulators for each antenna, it gives

$$C_{*\mathrm{MIMO}}(\boldsymbol{\alpha}) = \sum_{i=1}^{N_G} C_{*i}(\alpha_i). \tag{31}$$

Values α_i are square roots of the eigenvalues of $\mathbf{H}\mathbf{H}^H$, $\alpha_i = \sqrt{\lambda_i} = \sqrt{\mathrm{eig}_i(\mathbf{H}\mathbf{H}^H)}$. The index i denoting the particular eigenmode/antenna is *dropped* for the notation simplicity in the whole subsequent treatment. The symmetric capacity per one eigenmode is obtained from the mutual information expressed in terms of the entropy

$$C_*(\alpha) = I(\mathbf{s}_n; \mathbf{y}_n)|_{P_m = \frac{1}{M_c}} = \mathcal{H}[\mathbf{y}_n] - \mathcal{H}[\mathbf{w}_n]|_{P_m = \frac{1}{M_c}} \tag{32}$$

where $\mathcal{H}[\mathbf{w}_n] = N_h \log_2(2\pi N_0 e)$. The capacity depends on particular eigenvalue α.

4.2.3 Memoryless modulator—IID channel symbols

Dropping the details (see [9]), we get final expression for the symmetric capacity as

$$C_*(\alpha) = -\,\mathrm{E}[\log_2 \sum_{m=1}^{M_q} \frac{1}{M_c} p_{\mathbf{w}}(\mathbf{y}_n - \alpha \mathbf{s}^{(m)})] - \mathcal{H}[\mathbf{w}_n]. \tag{33}$$

4.2.4 Channel symbols as a Markov chain

Now we extend the previous results into the case when the modulator discrete part has *memory*. The channel symbols at one antenna (*dropping* the antenna index) depend on the data and modulator state $q_n = q(c_n, \sigma_n)$. The equivalent transmitted signal is then a function of the channel symbols $\mathbf{s}_n = \mathbf{s}(q_n)$. The sequence $\{q_n\}_n$ forms a *stationary* Markov chain. The mapping $q_n \mapsto \mathbf{s}_n$ for the individual eigenmode is also assumed to be a one-to-one mapping. The equivalent signal space representation of transmitted signal $\mathbf{s}_n$ also forms a Markov chain with the same transition matrix $\boldsymbol{\Pi}$. The output $\mathbf{y}_n$ of the equivalent channel model forms a *hidden* Markov chain.

The capacity evaluation in the case of the output sequence with hidden Markov property is somewhat more involved. Average mutual information per one symbol can be expressed as

function of *entropy rates* $\bar{I}(\mathbf{s}_n;\mathbf{y}_n) = \bar{\mathcal{H}}[\mathbf{y}_n] - \bar{\mathcal{H}}[\mathbf{w}_n]$. As a consequence of being white, the noise entropy rate is $\bar{\mathcal{H}}[\mathbf{w}_n] = \mathcal{H}[\mathbf{w}_n] = N_h \log_2(2\pi N_0 e)$. The entropy rate of the channel output can be lower and upper bounded [15]

$$\bar{\mathcal{H}}[\mathbf{y}_n] \geq \mathcal{H}[\mathbf{y}_n|\mathbf{y}_{n-1},\ldots,\mathbf{y}_1,\mathbf{y}_0,\mathbf{s}_0], \tag{34}$$

$$\bar{\mathcal{H}}[\mathbf{y}_n] \leq \mathcal{H}[\mathbf{y}_n|\mathbf{y}_{n-1},\ldots,\mathbf{y}_1,\mathbf{y}_0]. \tag{35}$$

The bounds approach the $\bar{\mathcal{H}}[\mathbf{y}_n]$ as n increases. However, the required dimensionality of integration when evaluating the conditional entropy also increases making this rather mathematically intractable. Therefore we use a *first order approximation*

$$\mathcal{H}[\mathbf{y}_1|\mathbf{y}_0,\mathbf{s}_0] \leq \bar{\mathcal{H}}[\mathbf{y}_n] \leq \mathcal{H}[\mathbf{y}_1|\mathbf{y}_0]. \tag{36}$$

Skipping details, we can get for these bounds $\mathcal{H}[\mathbf{y}_1|\mathbf{y}_0] = \mathcal{H}[\mathbf{y}_1]$ and

$$\mathcal{H}[\mathbf{y}_1|\mathbf{y}_0,\mathbf{s}_0] = -\int_{-\infty}^{\infty} \sum_{m=1}^{M_q} P_m \sum_{k=1}^{M_q} \Pi_{m,k}\, p_{\mathbf{w}}(\mathbf{y}_1 - \alpha\mathbf{s}^{(k)}) \log_2 \sum_{j=1}^{M_q} \Pi_{m,j}\, p_{\mathbf{w}}(\mathbf{y}_1 - \alpha\mathbf{s}^{(j)})\, d\mathbf{y}_1. \tag{37}$$

It is easy to see that the symmetric capacity Markov model *upper bound* (first order approximation) $C_*^{\mathrm{MUB}}(\alpha)$ is *equivalent* to the *memoryless case* $C_*^{\mathrm{MUB}}(\alpha) = C_*(\alpha)$ treated in the previous section. Unfortunately, this makes the bound rather loose since it completely ignores the memory. There is also, another *trivial finite alphabet upper bound* $C_*^{\mathrm{TUB}} = \log_2 M_c$ which holds *generally* for *arbitrary* (e.g., no envelope constraint) finite alphabet modulation. A combination of these two can be used to narrow the gap

$$C_*(\alpha) \leq C_*^{\mathrm{UB}}(\alpha) = \min\left(C_*^{\mathrm{TUB}}, C_*^{\mathrm{MUB}}(\alpha)\right). \tag{38}$$

The symmetric capacity *lower bound* of *one eigenmode* is

$$C_*^{\mathrm{MLB}}(\alpha) = \mathcal{H}[\mathbf{y}_1|\mathbf{y}_0,\mathbf{s}_0] - N_h \log_2(2\pi N_0 e)\big|_{P_m=\frac{1}{M_c}}. \tag{39}$$

4.2.5 Mean capacity for random channel

For random IID Rayleigh channel, the channel eigenvalues obey Wishart distribution [2]. But unlike from the continuous-valued channel input, the eigenmode capacity is expressed in terms of $\alpha_i = \sqrt{\lambda_i}$. The total average ergodic symmetric capacity for IID symbols (and similarly upper/lower bounds for the Markov case) is got by the averaging $\bar{C}_{*\mathrm{MIMO}} = N_H\, \mathrm{E}_\alpha[C_*(\alpha)]$ where $N_H = \min(N_T, N_R)$. The averaging E_α is done with respect to the one eigenmode *marginal* distribution from the *unordered* joint one. Clearly, the PDF is $p_\alpha(\alpha) = 2\alpha p_\lambda(\alpha^2)$ where

$$p_\lambda(\lambda) = \frac{1}{a}\sum_{k=0}^{a-1} \frac{k!}{(k+b-a)!}(L_k^{b-a}(\lambda))^2 \lambda^{b-a} e^{-\lambda}. \tag{40}$$

The function $L_k^a(.)$ is Laguerre polynomial, $a = \min(N_T, N_R)$, $b = \max(N_T, N_R)$.

4.2.6 Numerical results

The symmetric capacity behavior of the waveform and optionally memory constrained nonlinear modulation in MIMO channel is now demonstrated on examples. The linear modulation serves as a reference allowing to demonstrate the influence of higher dimensionality of nonlinear modulation. We chose *constant* symbol energy schemes. Examples share a common (2, 2)

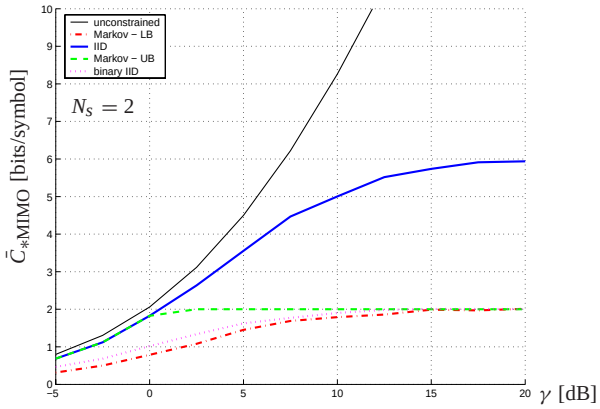

Figure 7: MSK waveforms ($N_s = 2$) in (2, 2) Rayleigh MIMO channel.

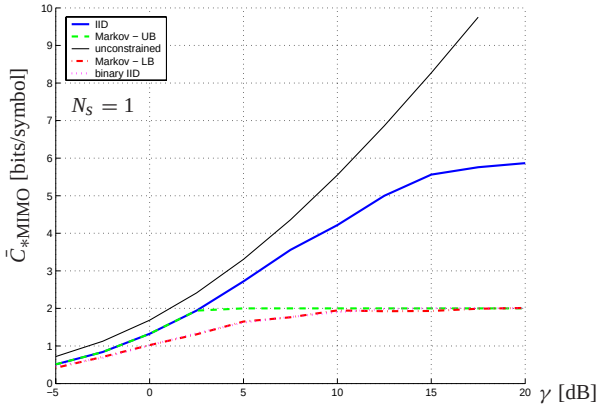

Figure 8: 8PSK waveforms ($N_s = 1$) in (2, 2) Rayleigh MIMO channel.

Rayleigh MIMO channel with rank $N_H = 2$. The mean received symbol energy to noise PSD ratio per one receiver is $\gamma = \mathrm{E}[\|\tilde{\mathbf{s}}\|^2]/(2N_0)$. We show also a result with *no input alphabet constrain* [12] with the same dimensionality N_s for a comparison. Integrations in the capacity expressions were evaluated by Monte Carlo method over the marginal eigenvalue. See Fig. 7 and 8 for the mean capacity results.

5 Trellis space-time coding for NSTM of CPM type

Design of the trellis code for NSTM of CPM type is (unlike for the linear modulations) very difficult task. The main problem arises from the fact that we need to synthesize trellis coder feeding the modulator subsystem having *inherent memory*. All space-time coder trellis transitions are therefore covered by additional layer of FSM from their impact on the transmitted signal. Here we discuss design rules for trellis coded CPM type space-time modulation in Rayleigh flat fading channel. For the details refer to [8].

5.1 Distance evaluation trellis

We have analyzed the mean squared distance of the trellis coded CPM type constant envelope space-time modulated signal in a Rayleigh slowly flat fading spatial diversity channel with independent coefficients. It is shown that the distance evaluation depends on both—the *modulator trellis* and on the *distance evaluation trellis*. The latter has a special properties regarding to its

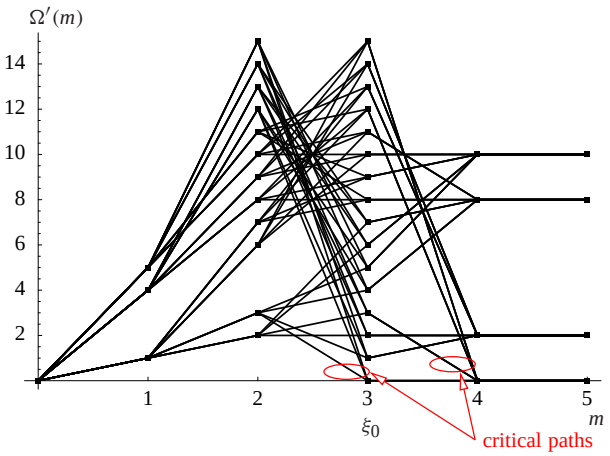

Figure 9: Example (RC2 CPM) of distance evaluation trellis with critical paths.

free paths. These properties—a *critical path* and the distance increments behavior are the basis for the space-time trellis code design. We identify the trellis code (data to channel phase symbols mapping) design rules minimizing the mean squared distance. The critical path is shown to be the determining factor. The overall procedure is general and is not exclusively related to the spatial channel. It can be applied to the design of a code which is applied to any modulation possessing itself a memory described by the finite state machine model.

5.2 NSTM-CPM trellis code design principle

The *design principle* can be summarized into the following steps: (1) search for terminating sequences, (2) classify them according to the length and determine the critical path in distance evaluation trellis, (3) exclude the critical sequences from the stock, (4) use the remaining ones for ST trellis code.

The first two steps related to the finding of critical paths are essential parts of the design procedure. They are found with utilization of the distance evaluation trellis. It can be shown that the distance evaluation is a procedure with memory described by distance evaluation trellis

$$\rho'^2 = \sum_{m=-\infty}^{\infty} \Delta\rho'^2(m, \Delta\mathbf{q}_m, \mathbf{\Theta}(m)) \tag{41}$$

where its input $\Delta\mathbf{q}_m = \mathbf{q}_m^{(1)} - \mathbf{q}_m^{(2)}$ is channel symbol difference and the distance evaluation state is $\mathbf{\Theta}(m)$. The final terminal state identifies the terminating sequences. We can show that squared distance increment is zero $\Delta\rho'^2(m) = 0$ if and only if $\mathbf{\Theta}(m) = \mathbf{0}$ and $\Delta\mathbf{q}_m = \mathbf{0}$. When the final state in the distance evaluation trellis is reached paths with the final state $\mathbf{\Theta}(m) = \mathbf{0}$ stop to increase the accumulated squared distance. On the other side the paths with the final state $\mathbf{\Theta}(m) \neq \mathbf{0}$ continue to increase the accumulated squared distance. An example of the distance evaluation trellis is on Fig. 9. Fig. 10 shows a simple 2-space 2-state ($M_\sigma = 2$) modulator trellis for binary data ($M_d = 2$) for RC2 CPM.

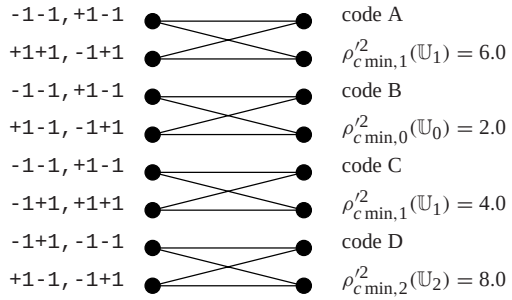

Figure 10: An example of 2-space 2-state ($M_\sigma = 2$) modulator trellis for binary data ($M_d = 2$) for the RC2 CPM. The vectors at the left hand side are the channel phase symbol vectors. The first is used for the upper and the second for the lower branch splitting at the given state.

6 Nonlinear Signal Processing for NSTM

6.1 Equivalent system model with composite coefficients

The transmitted signal passes through (N_T, N_R) MIMO flat fading channel. In our next treatment, the signal *preprocessing* (not actual space-time decoding) is done separately at each receive antenna. For the sake of notational clarity, the particular *index* of receive antenna will be *dropped* in the rest of the paper. The signal at arbitrary receive antenna consists of the useful signal $a(t)$ which is a weighted superposition of signals from all transmit antennas and the additive noise

$$x(t) = a(t) + w(t) \tag{42}$$

where we denote $x(t) = Xe^{j\psi}$. The noise $w(t)$ is the complex rotationally invariant white Gaussian noise passed through the receiver front-end selectivity (not affecting the useful signal) thus having finite variance σ_w^2 and zero mean. The useful signal is

$$a(t) = Ae^{j\alpha} = \sum_{i=1}^{N_T} h_i s_i(t, \mathbf{q}_i) = \sum_{i=1}^{N_T} A_i e^{j\alpha_i} = \sum_{i=1}^{N_T} a_i \tag{43}$$

where $h_i = H_i e^{j\eta_i}$ are channel coefficients and $\alpha_i = \phi_i + \eta_i$ are composite instant phases of the modulator ($s_i = e^{j\phi_i}$) and the channel, $A_i = H_i$, and $a_i = A_i e^{j\alpha_i}$. For the rest of the treatment, the channel coefficients h_i are assumed to be *known*. Assuming h_i is known, we can equivalently treat the equivalent system with composite (transmitted signal with channel) amplitudes A_i and phases α_i (see also Fig. 16).

In the remaining part of the chapter, we assume the system with $N_T = 2$ transmit antennas. The resulting equivalent system model (w.r.t. composite coefficients) for signal at arbitrary receive antenna is

$$x(t) = Xe^{j\psi} = Ae^{j\alpha} + w = A_1 e^{j\alpha_1} + A_2 e^{j\alpha_2} + w. \tag{44}$$

6.2 Information waveform manifold

The useful part $a(t)$ of received signal (44) forms a *curved (nonlinear) topological space, the manifold*. Since it is formed by the information carrying signal we call it *Information Waveform Manifold (IWM)*. A particular form of the IWM for CPM *constant envelope* class of modulation allows a novel approach to the signal processing compared to the traditional Euclidean signal space decomposition based one. The background of the IWM based preprocessing can be found in [16], [17], [18].

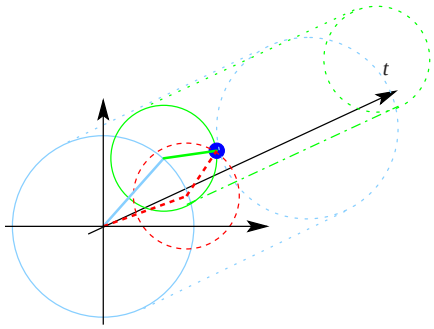

Figure 11: Two component CPM received signal IWM including two ambiguity modes (solid, dashed).

A particular form of the 2-component CPM signal IWM is a cylinder-on-cylinder (Fig. 11). Every manifold can be parametrized by its parametric space. The main *advantage* of the signal processing on IWM is two-fold.

1. The dimensionality of the parametric space of the IWM for 2-component CPM signal is equal to 3 (including time domain axis). The most obvious parametrization is $\{\alpha_1, \alpha_2, t\}$. This dimensionality does not depend on the particular CPM modulation type and it is typically much lower than the dimensionality of the traditional Euclidean signal space expansion.

2. The useful signal lies on known curved space. This opens a wide range of nonlinear processing possibilities not possible on traditional Euclidean signal space.

The concept of using the IWM receiver preprocessing consists of three basic steps.

1. Nonlinear projector on IWM.

2. Signal processing on the IWM (optional).

3. Isomorphism between IWM and decoder metric.

6.3 Nonlinear projector on IWM

The nonlinear projection operator $z(t) = T[x(t)]$ is the actual operation that reduces the dimensionality of the problem. It can be performed as operator, i.e. the mapping including the time domain, or as function $z(t) = T\,(x(t))$. The latter, called a *sampled* space projector, is generally suboptimal however much simpler. The full space projector can be replaced by the sampled one followed by a proper signal space processing on the IWM.

A particular form of sample space IWM projector for two component CPM signal can be based on *constrained ML* criterion [16]

$$z = \arg\max_{\check{a}\in\Psi} p(x|a) \tag{45}$$

where $\Psi = \{A_1 e^{j\alpha_1} + A_2 e^{j\alpha_2}\}_{\alpha_1,\alpha_2}$ is the useful signal IWM. The solution has a form of parametric limiter $z = \chi(X)e^{j\psi}$ with AM/AM conversion $Z = \chi(X)$ given by (see Fig. 12)

$$\chi(X) = \begin{cases} A_1 + A_2, & X > A_1 + A_2 \\ |A_1 - A_2|, & X < |A_1 - A_2| \\ X, & \text{elsewhere} \end{cases}. \tag{46}$$

Amplitudes A_1, A_2 are assumed to be known.

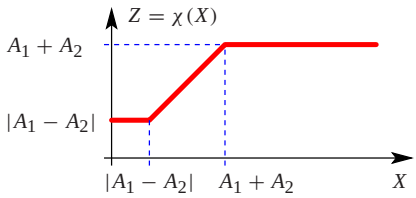

Figure 12: Parametric limiter.

6.4 Signal processing on the IWM

A signal processing on IWM is an optional step. It can replace true full IWM projection operator properly utilizing the properties of time-domain behavior of the signal on IWM. The signal processing on IWM must use tools from the differential geometry ([19], [20], [21], [22]) to perform the signal processing operations (intrinsic vs. extrinsic operations). The IWM is a curved space. The curvature generally stems from two sources. The first is a nonlinearity of phase function $\beta(t)$ in time. The second appears specifically in MIMO system where superposition of two cylindrical IWMs of CPM curves the space. A linear movement of the point on parametric space (phases α_i) of NSTM-CPM corresponds to a curved movement with generally non-constant curve velocity on the IWM. See [16] for details.

Assume a parametrized curve $\ell(\xi)$ which lies in the manifold Ψ which is embedded in the Euclidean space. The length of the curve in the manifold between two points $\ell(\xi_1), \ell(\xi_2)$ is defined as

$$\rho(\ell(\xi_1), \ell(\xi_2)) = \int_{\xi_1}^{\xi_2} \|\dot{\ell}(\xi)\| \, d\xi \tag{47}$$

where $\dot{\ell}(\xi)$ is the velocity vector of the curve.

One of the simplest signal processing tools is the sample mean. Although it is simple, it provides a nice insight into the problem of the signal processing on the IWM with application on NSTM. Assume we are given points $\{a_i\}_{i=1}^{N_a}$ on the manifold Ψ. We define *Intrinsic Sample Mean* as

$$\bar{a}_{\text{int}} = \arg\min_{a \in \Psi} \sum_i \rho^2(a, a_i). \tag{48}$$

Traditional mean calculated in the Euclidean space using ordinary Euclidean distance is called *Extrinsic Sample Mean*

$$\bar{a}_{\text{ext}} = \arg\min_{a \in \Psi} \sum_i \|a - a_i\|^2. \tag{49}$$

The extrinsic mean can be also interpreted as an evaluation of the average value in Euclidean space $\frac{1}{N_a}\sum_i \|a - a_i\|^2$ with subsequent projection of this value on the manifold Ψ. The intrinsic and extrinsic values can substantially differ. The intrinsic value fully utilizes the knowledge of the shape of the manifold including the possibly nonuniform velocity of the curve.

Example

In order to demonstrate the impact of the intrinsic evaluation, we consider this very simple example which relates directly to the possible processing of the CPM class NSTM in MIMO channel with additive noise. Assume two constant envelope signals with know magnitudes A_1, A_2 in additive noise ζ. The signal point is $z = A_1 e^{j\alpha_1} + A_2 e^{j\alpha_2} + \zeta$. The IWM of this example is the parametric space $\Psi = \{A_1 e^{j\alpha_1} + A_2 e^{j\alpha_2}\}_{\alpha_1,\alpha_2}$. Assume for the simplicity that the signal z is already projected on the manifold Ψ, i.e. $z \in \Psi$ (noise term ζ is generally different from w). Our goal is to average the sequence of the observations $\{z_i\}_i$ (e.g. the samples) of the

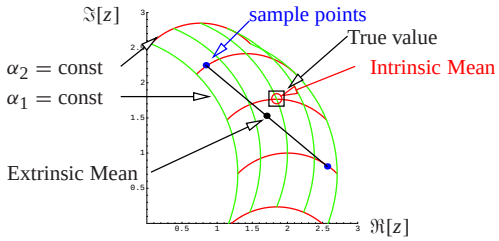

Figure 13: Example of the evaluation of intrinsic and extrinsic mean.

signal z. The evaluated intrinsic and extrinsic mean is shown on Fig. 13. We used $A_1 = 1$, $A_2 = 2$ and the sample points z_i intentionally chosen such that their intrinsic mean is equal to the true value. There are also shown the curves of $\alpha_1 = \text{const}$ and $\alpha_2 = \text{const}$ with equidistant (intrinsic) increments. □

6.5 Isomorphism between IWM and decoder metric

At the end of IWM processing, we must provide a suitable metric for the outer space-time decoder. This isomorphism can have various forms depending on the particular needs of space-time decoder.

The decoding metric composed of individual component phase estimates is clearly one of the attractive choices. The isomorphism can be constructed using a geometric approach (solving the triangular problem) [16] where we assume that the $Ae^{j\alpha}$ is already on the IWM. The solution has generally two ambiguity domains $[\hat{\alpha}'_1 - \alpha, \hat{\alpha}'_2 - \alpha] \in \left\{\pm[\check{\alpha}'_1, \check{\alpha}'_2]\right\}$ where ($\check{\alpha}'_1 \in [0, -\pi]$, $\check{\alpha}'_2 \in [\pi, 0]$)

$$\check{\alpha}'_1 = -\arccos\left(\left(A_1^2 - A_2^2 + A^2\right) / (2A_1A)\right), \tag{50}$$

$$\check{\alpha}'_2 = \arccos\left(\left(A_2^2 - A_1^2 + A^2\right) / (2A_2A)\right). \tag{51}$$

6.6 2-Component IWM Phase Discriminator

The particular form of IWM receiver preprocessing is the 2-Component IWM Phase Discriminator. It consists of nonlinear sample space projector on IWM implemented as parametric limiter (46) and decoder metric formed as estimates of composite phases α_1, α_2 for the actual *projected* point of the *received* signal $z = Ze^{j\psi}$ (using the geometric approach). The solution is $[\hat{\alpha}_1 - \psi, \hat{\alpha}_2 - \psi] \in \left\{\pm[\check{\alpha}_1, \check{\alpha}_2]\right\}$ where ($\check{\alpha}_1 \in [0, \pi]$, $\check{\alpha}_2 \in [-\pi, 0]$)

$$\check{\alpha}_1 = -\arccos\left(\left(A_1^2 - A_2^2 + Z^2\right) / (2A_1Z)\right), \tag{52}$$

$$\check{\alpha}_2 = \arccos\left(\left(A_2^2 - A_1^2 + Z^2\right) / (2A_2Z)\right). \tag{53}$$

One of the problems of the solutions (52), (53) is the two-fold ambiguity. The Fig. 14 (a) clearly shows that ambiguity free solution (solution 1 chosen) of the triangular problem is defined by condition for the true composite phases

$$\alpha_1 < \alpha_2 < \alpha_1 + \pi, \quad \alpha_1 \in [0, 2\pi). \tag{54}$$

This is shown on Fig. 14 (b). The solution for real received signal is then

$$\hat{\alpha}_1 = \psi - \arccos\left(\left(A_1^2 - A_2^2 + Z^2\right) / (2A_1Z)\right), \tag{55}$$

$$\hat{\alpha}_2 = \psi + \arccos\left(\left(A_2^2 - A_1^2 + Z^2\right) / (2A_2Z)\right). \tag{56}$$

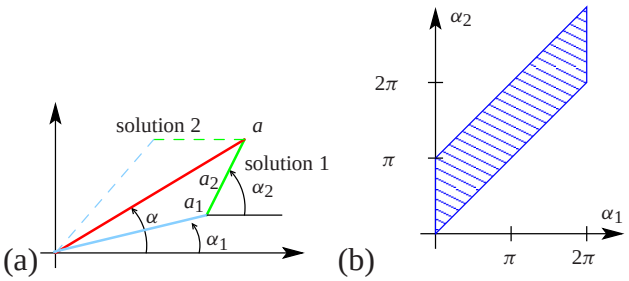

Figure 14: (a) Ambiguous solution of the triangular problem. (b) Ambiguity-free region for solution 1.

The ambiguity free region (54) at the level of composite phases α_i can be equivalently achieved by a correct ambiguity resolution using proper precoding at the transmitter side (restricting the values of ϕ_i) and by assuming the known channel coefficients. For the rest of the chapter, we will assume that the composite phases *fulfill* the condition (54) which is equivalent to the perfect *ambiguity resolution*.

6.7 Information sufficiency of the nonlinear projector

The projector generally does not form a sufficient statistic [16]. In the ideal case, the projector should have a property of sufficient statistic, i.e. it should preserve the information contents of the channel symbols $I(\tilde{\mathbf{q}}; x(t)) = I(\tilde{\mathbf{q}}; z(t))$. The sufficiency condition at the level between *instant* (sampled) phases $\boldsymbol{\alpha} = [\alpha_1, \ldots, \alpha_{N_T}]^T$ and the *sampled* channel output x (ESWS) or projector output z (ISWM) is generally stronger but somewhat easier to evaluate $I(\boldsymbol{\alpha}; x) = I(\boldsymbol{\alpha}; z)$. This will be further considered.

The sufficiency condition is not generally fulfilled. Even in the simplest case of SISO single component CPM in AWGN ($x = Ae^{j\alpha} + w$) complete value (magnitude and phase) $x = Xe^{j\psi}$ is needed. From the Neyman-Fisher factorization theorem for the sufficient statistic, it can be inferred easily that the magnitude X and phase ψ in

$$p(x|\alpha) = \frac{1}{\pi\sigma^2} e^{-\frac{X^2 + A^2 - 2XA\cos(\psi - \alpha)}{\sigma^2}} \tag{57}$$

cannot be decoupled for the α estimation. The phase alone is not the sufficient statistic. Independence of the stationary point on the X is not enough, see [23]. Therefore, it is a legitimate question what is the information loss $I(\boldsymbol{\alpha}; x)/I(\boldsymbol{\alpha}; z)$ caused by a particular projector.

A numerical evaluation of the sufficiency condition by comparing $I(\boldsymbol{\alpha}; x)$ and $I(\boldsymbol{\alpha}; z)$ for various values A_1, A_2 (Fig. 15) shows a negligible loss of information at the low signal to noise region. In the high signal to noise region, the loss tends to zero. Signal to noise ratio is defined as $\sum_i A_i^2/\sigma^2$. Notice that the particular case of $A_1 = 1$, $A_2 = 0$ corresponds to a scalar (SISO) hard-limiter receiver.

6.8 Multiplexing Properties of the Discriminator

A constant envelope CPM class of NSTM modulations at multi-antenna transmitter is considered. Each receive antenna in MIMO system receives a superposition of CPM waveforms. The useful signal at the receiver spans a curved space —IWM. Particularly it has a form of a cylinder on cylinder for 2-component CPM signal. At the receiver, we use a nonlinear preprocessor consisting of nonlinear projector on the IWM, optional processing on curved space and decoding

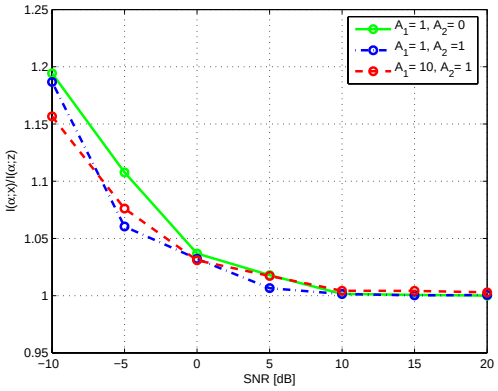

Figure 15: Ratio of the mutual information for the ESWS observation $I(\boldsymbol{\alpha}; x)$ and the projection on ISWM $I(\boldsymbol{\alpha}; z)$.

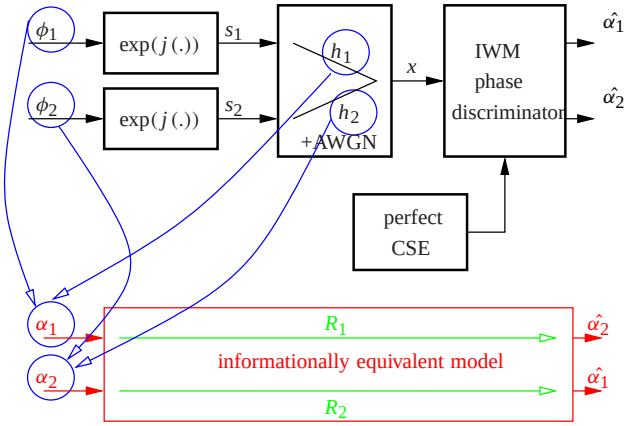

Figure 16: System model of multiplexing IWM processing at one receive antenna.

isomorphism. A particular form of the preprocessor, the 2-component IWM phase discriminator, is analyzed. We show that the discriminator can *separate individual instant phases* of the component CPM modulations and therefore has multiplexing capabilities with respect to the individual transmitted components. It creates parallel eigen-space like virtual channels. No time domain processing is needed, the procedure fully relies on the curved space properties of the IWM and thus is applicable with arbitrary outer space-time coding of NSTM-CPM. Information theoretic analysis of the multiplexing properties based on capacity region is presented. We show that the discriminator provides good separation of component phases.

6.8.1 Multiplexing IWM processing

The information carrying phases $\phi_i(t, \mathbf{q}_i)$ are separated at receiver (at the level of composite phases $\alpha_i = \phi_i + \eta_i$) thus allowing information multiplexing of the individual data $\mathbf{q}_i$ streams (see Fig. 16). It is very *important* to stress that the whole *multiplexing processing* of the IWM discriminator is purely done in *value domain without any time-domain processing*. Therefore it is easily applicable with arbitrary outer space-time coding performed on phases ϕ_i.

6.8.2 Capacity region

The *informationally equivalent* system on the Fig. 16 is a system with two inputs α_1, α_2 (informationally equivalent inputs get from the knowledge of channel h_1, h_2 and ϕ_1, ϕ_2) and two

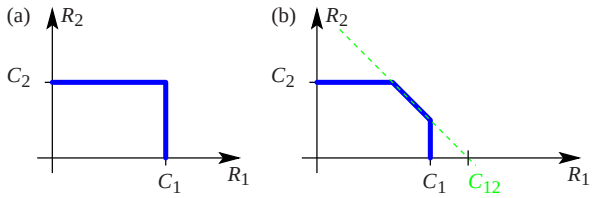

Figure 17: Capacity region with (a) perfect multiplexing (separation), (b) imperfect multiplexing.

outputs $\hat{\alpha}_1, \hat{\alpha}_2$. Let the R_i be the information rate between $\{\alpha_i, \hat{\alpha}_i\}$ defined separately for $m \in \{1, 2\}$. The bounding conditions for these rates are given by capacity region

$$R_1 < C_1 = I(\alpha_1; \hat{\alpha}_1|\alpha_2), \tag{58}$$
$$R_2 < C_2 = I(\alpha_2; \hat{\alpha}_2|\alpha_1), \tag{59}$$
$$R_1 + R_2 < C_{12} = I(\boldsymbol{\alpha}; \hat{\boldsymbol{\alpha}}), \tag{60}$$

where $\boldsymbol{\alpha} = [\alpha_1, \alpha_2]^T$ and $\hat{\boldsymbol{\alpha}} = [\hat{\alpha}_1, \hat{\alpha}_2]^T$. This capacity region is somewhat similar to that of classical multiple access channel (see [15]). It has however one subtle but *important difference*. The conditional mutual information in (58) and (59) has the output variable corresponding only to *one of the output*, unlike as it is in multiple access case where both of them are considered. The mutual information interpretation is the amount of information shared between single input and single output given that the other one is not present or it is known (which is equivalent — any of its influence can be subtracted). This is obviously the most favorable situation and the rate R_i cannot exceed this value under any condition. The sum-rate condition evaluates the total information throughput between both inputs jointly and both outputs where encoder and decoder can use joint processing for both channels.

The capacity region allows to quantitatively asses the multiplexing properties of the system, i.e. the level of separation of the virtual channels $\hat{\alpha}_1(\alpha_1)$ and $\hat{\alpha}_2(\alpha_2)$. The situation is demonstrated on Fig. 17. The perfect multiplexing allows communication in channel $\hat{\alpha}_1(\alpha_1)$ on the rate R_1 without any influence of the rate R_2 in the second channel (and similarly vice versa).

We define the *multiplexing separation ratio* as

$$\kappa = \frac{C_{12}}{C_1 + C_2}. \tag{61}$$

Clearly, any value $\kappa < 1$ causes the capacity region (Fig. 17) to have upper right corner cut-out by C_{12} condition. This corresponds to imperfect channel separation. The coefficient κ describes a quality of channel separation, the lower κ the worse separation.

6.8.3 Approximation of the discriminator output

The evaluation of the quantities C_1, C_2, C_{12} in an exact manner is intractable. The difficulty arises from two sources. The first is nonlinear projector $z = \chi(X)e^{j\psi}$ and the second one comes from the nonlinear functions in (55), (56). Therefore we first try to find tractable approximation of the discriminator output.

Both problems can be overcome assuming medium to large signal-to-noise ratio. In this case the information loss caused by nonlinear projector is negligible [16]. We can then approximate the solution by leaving out the projector and assuming that the noise level will be such that conditions for solution existence hold. As a next step we can linearize the estimation error

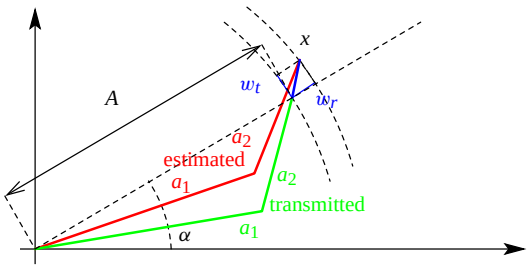

Figure 18: Tangential and radial noise components.

evaluation using proper evaluation of its tangential w_t and radial w_r components. See Fig. 18. Skipping the details (see [18]) we get *linearized estimation error* as

$$\Delta\alpha_1 = \frac{w_t}{A} + w_r \frac{A^2 - A_1^2 + A_2^2}{2A^2 A_1 \sqrt{1 - \frac{(A^2 + A_1^2 - A_2^2)^2}{4A^2 A_1^2}}}, \tag{62}$$

$$\Delta\alpha_2 = \frac{w_t}{A} - w_r \frac{A^2 + A_1^2 - A_2^2}{2A^2 A_2 \sqrt{1 - \frac{(A^2 - A_1^2 + A_2^2)^2}{4A^2 A_2^2}}}. \tag{63}$$

We denote $\hat{\tilde{\boldsymbol{\alpha}}} = [\hat{\tilde{\alpha}}_1, \hat{\tilde{\alpha}}_1]^T$ and $\boldsymbol{\alpha} = [\alpha_1, \alpha_2]^T$.

6.8.4 Approximation of the capacity region

The linearized discriminator model can be now used for evaluation of C_1, C_2, C_{12}. The linearized estimation error $\Delta\boldsymbol{\alpha} = [\Delta\alpha_1, \Delta\alpha_2]^T$ has conditional PDF[1] $p_{\Delta\boldsymbol{\alpha}|\boldsymbol{\alpha}}(\Delta\boldsymbol{\alpha})$ which is zero mean Gaussian with covariance matrix

$$\mathbf{C}_{\Delta\boldsymbol{\alpha}} = \frac{\sigma_w^2}{2} \frac{\begin{bmatrix} -4A_2^2 & 2(A^2 - A_1^2 - A_2^2) \\ 2(A^2 - A_1^2 - A_2^2) & -4A_1^2 \end{bmatrix}}{A^4 + (A_1^2 - A_2^2)^2 - 2A^2(A_1^2 + A_2^2)}. \tag{64}$$

The covariance is inherently a function of composite phases $\mathbf{C}_{\Delta\boldsymbol{\alpha}}(\boldsymbol{\alpha})$ through the variable $A(\boldsymbol{\alpha})$.

Capacities obtained from the linearized estimation model are

$$\tilde{C}_i = I(\hat{\tilde{\alpha}}_i; \alpha_i | \bar{\alpha}_i) = \mathcal{H}[\hat{\tilde{\alpha}}_i | \bar{\alpha}_i] - \mathcal{H}[\hat{\tilde{\alpha}}_i | \boldsymbol{\alpha}], \tag{65}$$

$$\tilde{C}_{12} = I(\hat{\tilde{\boldsymbol{\alpha}}}; \boldsymbol{\alpha}) = \mathcal{H}[\hat{\tilde{\boldsymbol{\alpha}}}] - \mathcal{H}[\hat{\tilde{\boldsymbol{\alpha}}} | \boldsymbol{\alpha}] \tag{66}$$

where $\mathcal{H}[\mathbf{.}]$ is the entropy, $i \in \{1, 2\}$, and $\bar{\alpha}_i$ is a complementary input for α_i (e.g. $\bar{\alpha}_1 = \alpha_2$). The multiplexing separation ratio for linearized model is $\tilde{\kappa} = \tilde{C}_{12}/(\tilde{C}_1 + \tilde{C}_2)$.

Capacities are evaluated with the input distribution of $\boldsymbol{\alpha}$ with independent components with *uniform* distribution over the *ambiguity-free region* (Fig. 14) and *Gaussian* linearized estimation error. Details of the mutual information evaluation are shown in [18].

A numerical evaluation of capacity region, $\tilde{C}_1, \tilde{C}_2, \tilde{C}_{12}$ and $\tilde{\kappa}$ are shown on Fig 19, Fig 20, Fig 21. A signal to noise ratio is defined as $\Gamma = \sum_i A_i^2/\sigma_w^2$. We see that the *multiplexing separation* is very *good* in most cases.

[1] Probability density function.

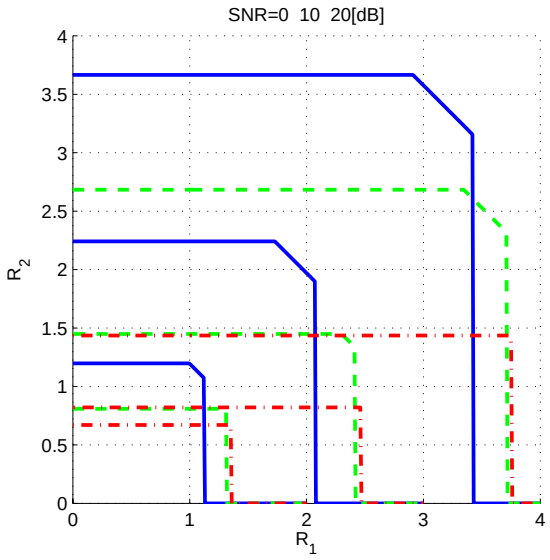

Figure 19: Capacity region of linearized estimation model. (a) $A_1 = 1,\ A_2 = 1$ solid line, (b) $A_1 = 3,\ A_2 = 1$ dashed line, (c) $A_1 = 10,\ A_2 = 1$ dash-dotted line.

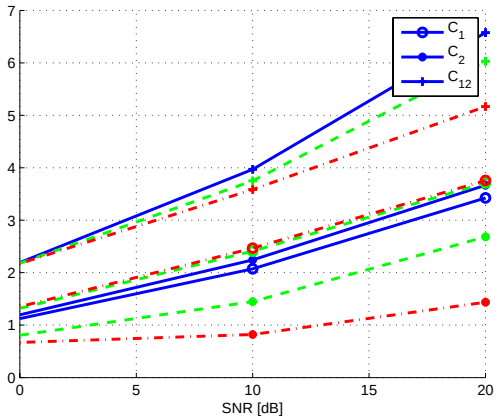

Figure 20: Capacities $\tilde{C}_1, \tilde{C}_2, \tilde{C}_{12}$ of linearized estimation model. (a) $A_1 = 1,\ A_2 = 1$ solid line, (b) $A_1 = 3,\ A_2 = 1$ dashed line, (c) $A_1 = 10,\ A_2 = 1$ dash-dotted line.

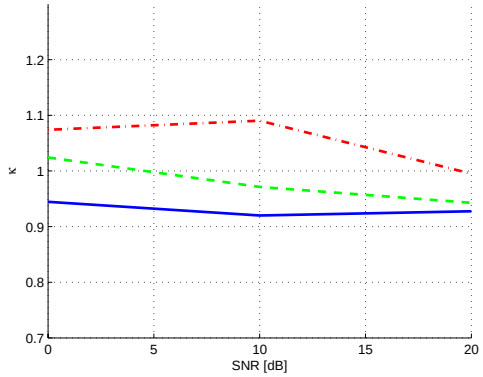

Figure 21: Multiplexing separation ratio $\tilde{\kappa}$ of linearized estimation model. (a) $A_1 = 1,\ A_2 = 1$ solid line, (b) $A_1 = 3,\ A_2 = 1$ dashed line, (c) $A_1 = 10,\ A_2 = 1$ dash-dotted line.

References

[1] B. Vucetic and J. Yuan, *Space-Time Coding*. John Wiley & Sons, 2003.

[2] I. E. Telatar, "Capacity of multi-antenna Gaussian channels," tech. rep., Lucent Technologies, 1995. http://mars.bell-labs.com/cm/ms/what/mars/.

[3] M.-S. Alouini and A. J. Goldsmith, "Capacity of Rayleigh fading channels under different adaptive transmission and diversity-combining techniques," *IEEE Trans. Veh. Technol.*, vol. 48, pp. 1165–1181, July 1999.

[4] V. Tarokh, N. Seshadri, and A. R. Calderbank, "Space-time codes for high data rate wireless communication: Performance criterion and code construction," *IEEE Trans. Inf. Theory*, vol. IT-44, pp. 744–765, Mar. 1998.

[5] E. G. Larsson and P. Stoica, *Space-Time Block Coding for Wireless Communications*. Cambridge University Press, 2003.

[6] X. Zhang and M. P. Fitz, "Space-time code design with continuous phase modulation," *IEEE J. Sel. Areas Commun.*, vol. 21, pp. 783–792, June 2003.

[7] X. Zhang and M. P. Fitz, "Symmetric information rate for continuous phase channel and BLAST architecture with CPM MIMO system," in *Proc. IEEE Internat. Conf. on Commun. (ICC)*, 2003.

[8] J. Sykora, "Constant envelope space-time modulation trellis code design for Rayleigh flat fading channel," in *Proc. IEEE Global Telecommunications Conf. (GlobeCom)*, (San Antonio, TX, USA), pp. 1113–1117, Nov. 2001.

[9] J. Sykora, "Symmetric capacity of nonlinearly modulated finite alphabet signals in MIMO random channel with waveform and memory constraints," in *Proc. IEEE Global Telecommunications Conf. (GlobeCom)*, (Dallas, USA), pp. 1–6, Dec. 2004.

[10] J. Sýkora, *Teorie digitální komunikace (Theory of Digital Communications (in Czech))*. Praha: vydavatelství ČVUT, Feb. 2002.

[11] J. G. Proakis, *Digital Communications*. McGraw-Hill, 4th ed., 2001.

[12] J. Sykora, "MIMO spatial diversity communications—signal processing and channel capacity," *Radioengineering*, vol. 11, pp. 6–11, Dec. 2002.

[13] P. A. Laurent, "Exact and approximate construction of digital phase modulations by superposition of amplitude modulated pulses (AMP)," *IEEE Trans. Commun.*, vol. COM-34, pp. 150–160, Feb. 1986.

[14] J. Sykora, "Information capacity of nonlinearly modulated finite alphabet signals in MIMO channel," in *COST 273 MCM*, (Paris, France), pp. 1–7, May 2003. TD-03-094.

[15] T. M. Cover and J. A. Thomas, *Elements of Information Theory*. John Wiley & Sons, 1991.

[16] J. Sykora, "Information waveform manifold based preprocessing for nonlinear multichannel modulation in MIMO channel," in *Proc. IEEE Global Telecommunications Conf. (GlobeCom)*, (St. Louis, USA), pp. 1–6, Nov. 2005.

[17] J. Sykora, “Linear subspace projection and information waveform manifold based preprocessing for nonlinear multichannel modulation in MIMO channel,” in *Proc. Int. Conf. on Telecommunications (ICT)*, (Cape Town, South Africa), pp. 1–6, May 2005. Invited paper.

[18] J. Sýkora, “Nelineární zpracování signálu mnohokanálových CPM modulací v MIMO kanálu,” *Slaboproudý obzor*, vol. Vol-61, no. 3, pp. 1–6, 2005.

[19] J. Xavier and V. Barroso, “New statistical bound for inference problems on Riemannian manifolds,” in *Proc. IEEE Workshop on Signal Processing Adv. in Wireless Commun. (SPAWC)*, 2004.

[20] J.-C. Belfiore, “Constructive coding on the Grassmann manifold: Application to non coherent space-time communication,” in *Proc. IEEE Workshop on Signal Processing Adv. in Wireless Commun. (SPAWC)*, 2004.

[21] A. Srivastava, “Bayesian estimation and tracking of dynamic signal subspaces,” in *Proc. IEEE Workshop on Signal Processing Adv. in Wireless Commun. (SPAWC)*, 2004.

[22] G. Lebanon, “Axiomatic geometry of conditional models,” *IEEE Trans. Inf. Theory*, vol. 51, Apr. 2005.

[23] S. M. Kay, *Fundamentals of Statistical Signal Processing: Estimation Theory*. Prentice-Hall, 1993.

doc. Ing. Jan Sýkora, CSc.

Czech Technical University in Prague
Faculty of electrical engineering
department of radioelectronics K13137
Technická 2, 166 27 Praha 6
Czech Republic

E-mail:Jan.Sykora@fel.cvut.cz
http://radio.feld.cvut.cz/˜sykora/

doc. (associate professor) (2002) CTU in Prague, FEE

CSc. (Ph.D.) (1993) CTU in Prague, FEE

Ing. (M.Sc. Eng.) (1987) CTU in Prague, FEE

Current position

associate professor (since 2002) at CTU in Prague, FEE, dept. of radioelectronics.

Previous positions

assistant professor (1991 – 2002) at CTU in Prague, FEE, dept. of radioelectronics.

PhD (1987 – 1991) at CTU in Prague, FEE, dept. of radioelectronics.

Research activity

- General research areas

  Digital communications theory — modulation, coding, signal processing algorithms at physical layer. Information theory in digital communications. Parameter estimation and detection theory. Statistical signal processing.

- Specific research areas

  Spatial diversity MIMO (Multiple-Input Multiple-Output) communication systems. Nonlinear space-time modulation and coding. Nonlinear space-time signal processing. Iterative detection, synchronization and equalization. Adaptive communication systems with specific constraints.

Projects, grants

2005–2007 GACR 102/05/2177 „Multiple-Input Multiple-Output spatial diversity mobile radio communication systems“

2005 industrial project, Dicom, sro., „PR20/SHARON (SHort rAnge Radio Operational Network), Digital radio communications system in 2.4 GHz” MultiBand Space-Time Coded OFDM with Time/Frequency Hopping.

2002–2004 GACR 102/02/0483 „Spatial diversity and adaptive digital communication systems“

2002–2005 MSMT (OC 273.001) „Physical layer signal processing algorithms for high speed mobile radio communication systems“

2001–2005 EU COST 273 „Towards mobile broadband multimedia networks“

1998–2000 GACR 102/98/1464 „Application of digital signal processing in radioelectronics“

1995–1998 EC Copernicus 708 project „Advanced Transmission and network management techniques in integrated satellite/terrestrial mobile systems“

1993–1995 EC COST project 227 „Terrestrial and Space Communication Networks“

Teaching activity

Digital communication theory, parameter estimation theory and signal processing theory with application to communication systems

Courses

Theory of Digital Communication (37TDK), Synchronization and Equalization (37SEK, X37SEK), Signals and Systems (E-SAS) [in English], Digital communications 1 (X37DK1), Digital communications 2 (X37DK2), Statistical signal processing (P37SZS), Radioelectronics and acoustics research seminars (P37VRA)

Professional affiliations

IEEE Communications Society, IEEE Information Theory Society, IEEE Signal Processing Society, IEEE Vehicular Technology Society

Professional service

Reviewer

IEEE Transactions on Communications, IEEE Communications Letters, IEEE Transactions on Wireless Communications, IEEE Transactions on Signal Processing, European Transactions on Telecommunications, IEE Proceedings - Communications, IEE Electronics Letters, Radioengineering

Conference Technical Program Committee

European Wireless 2007, IEEE ISWCS 2006, IEEE VTC 2007Spring, 2006Fall, 2006Spring, IEEE APCC 2005, Poster 2002–2006.

Committees at CTU

Doctoral Degree Program Committee at CTU FEE - Radioelectronics